# 基于晶体拉曼转换的多波长激光技术综述 (特邀)

吕志伟[1,2], 刘钟泽[1,2], 陈　晖[1,2], 金　舵[1,2], 郝　鑫[1,2], 范文强[1,2], 王雨雷[1,2], 白振旭[1,2*]

(1. 河北工业大学 先进激光技术研究中心，天津 300401；
2. 河北省先进激光技术与装备重点实验室，天津 300401)

**摘　要**：近年来, 在光电对抗、激光雷达、精密测量、医疗等诸多应用的牵引下, 能够同时或交替输出不同波长的激光器得到广泛关注, 但是受到激光工作物质中激活粒子固有发射谱及其增益强度的限制, 实现多波长激光的功率、波长和时频域的高效可控辐射具有较大难度。非线性光学频率变换技术是拓展激光波长的有效手段, 具有系统灵活性强、波长调节范围宽和功率拓展性强等特点。作为一种三阶非线性光学效应, 受激拉曼散射 (SRS) 通过介质内部的分子或晶格振动使入射的泵浦光产生一定的频移, 结合其固有的放大、相位共轭、级联转换等特性, 基于 SRS 的拉曼激光器在获得高功率、高光束质量、多波长激光输出中具有显著优势, 尤其是以晶体作为拉曼增益介质的多波长激光器一直是激光领域研究的热点。文中介绍了 SRS 和级联拉曼转换的基本原理, 归纳了典型晶体拉曼激光器的分类和基本结构, 综述并讨论了基于晶体拉曼转换的多波长激光技术的研究现状。

**关键词**：受激拉曼散射；　多波长激光；　拉曼晶体；　级联转换；　拉曼振荡器
**中图分类号**：TN248.1　　**文献标志码**：A　　**DOI**：10.3788/IRLA20230420

## 0　引　言

激光自 20 世纪问世以来, 以其卓越的方向性、相干性、单色性及高亮度等特性得到人们的广泛关注, 而激光技术的发展也极大地推动了科学研究、国防、医疗、工业等诸多领域和行业的革新。波长是激光光束的重要参数之一, 对激光器的应用起到至关重要的作用, 例如, 可见光波段激光常用于数据存储、光通信和新一代显示技术等领域[1−5], 近红外波段激光常用于激光武器、临床手术、精密加工和加密通讯等领域[6−10], 中长波红外激光波段常用于大气光谱检测和红外光电对抗[11−15]。当然, 激光的应用通常并不局限于某一个特定的波段, 如大气透过窗口在紫外、可见光和红外波段均有所覆盖[14,16], 针对不同材料和加工需求也通常采用不同波长的激光[17−18]; 在某些特定领域的应用中, 有时也需要激光工作在某个特定波长且具有满足特定的线宽, 如钠导星需要 589 nm 波长的窄线宽激光[19−20]。

近年来, 激光技术的发展不断推动医学眼底治疗、精密测量、雷达等方面逐步实现质的飞跃, 单一波长激光器已难以满足更高的应用需求, 多波长激光光源研制和应用已逐渐成为研究的热点 (图 1)[21−31]。在医学领域, 多波长激光治疗仪可针对眼底病变的程度与范围进行分区治疗 [9,22,32]。在通信领域, 波分复用技术的快速发展通常要求产生光源具有波长间隔小、线宽窄、功率谱平坦等特点, 其中较为典型的光源就是掺铒多波长激光器[33−34]。在科研领域, 利用非线性光学晶体将两个波长相近的激光进行混频成为产生太赫兹波的重要技术路径之一, 由于需要进行相位锁定, 因此利用单一光源直接产生双波长激光的稳定性要优于采用两台独立波长的激光器[35−36]。此外, 多波长激光器常用于差分吸收雷达、干涉彩虹全息等, 同时也在军事、智能装备等领域有着重要应用[37−40]。

**收稿日期**:2023−07−07;　**修订日期**:2023−08−02
**基金项目**:国家自然科学基金项目 (61927815); 天津市自然科学基金项目 (22JCYBJC01100, 20JCZDJC00430); 量子光学与光量子器件国家重点实验室开放课题项目 (KF202201); 河北工业大学基本科研业务费项目 (JBKYTD2201)
**作者简介**:吕志伟, 男, 教授, 博士生导师, 博士, 主要从事高功率激光技术与非线性光学方面的研究。
**通讯作者**:白振旭, 男, 教授, 博士生导师, 博士, 主要从事高功率激光技术与新型激光器方面的研究。

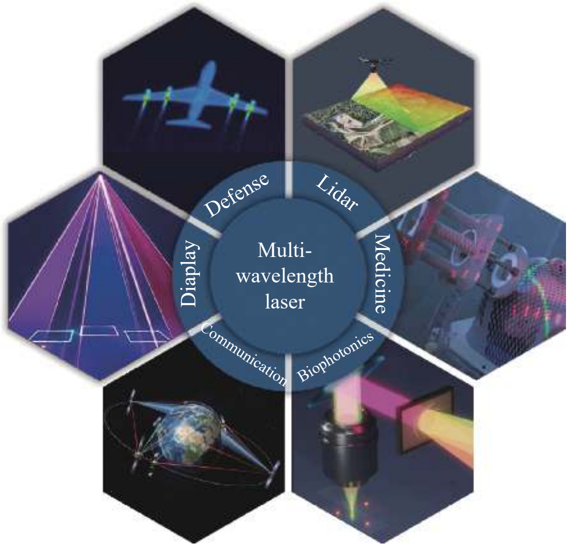


图 1 多波长激光器的典型应用[27-31]

Fig.1 Typical applications of multi-wavelength lasers [27-31]

常见实现多波长激光输出的方法包括: 利用工作物质固有的多条发射谱线直接实现多波长辐射、利用光栅等器件将不同波长激光进行光束合成、通过非线性光学频率变换将单一波长拓展至若干个波长等。利用工作物质直接辐射包括通过激活离子不同能带之间的跃迁产生大频率间隔的多波长激光, 或通过相同能带不同能级间的跃迁产生小频率间隔的多波长激光[41]。为克服工作物质的增益竞争, 往往需要控制谐振腔中不同跃迁谱线的损耗以达到目标波长的激发阈值, 如调节腔镜的透过率、谐振腔内损耗 (如插入标准具、滤光片等)、改变受激发射截面的大小等。人们现已实现 546 nm/550 nm[42]、1 061 nm/1 064 nm[43]、1 074 nm/1 112 nm[44]、1 112 nm/1 116 nm/1 123 nm[45] 以及 2 064 nm/2 066 nm[46] 等不同组合的多波长激光。但是不同发射波长之间增益竞争的存在, 使得基于单一工作物质的多波长激光器的输出参数往往难以实现理想调控。光束合成技术是将若干独立输出的不同波长激光通过分光或衍射等器件合成一束激光, 其特点在于参与合成的各光源参数独立控制, 避免了单一工作物质实现多波长运转出现的增益竞争[47−50]。近年来, 人们已经实现了诸多不同频率和波长间隔的高功率光束合成输出[51−53]。光束合成技术的难点在于系统结构较为复杂, 且通过空间组合的方式难以实现多波长光束的同轴输出。非线性光学频率变换技术可获得丰富波长的辐射, 是目前获得多波长激光输出的重要途径, 常见的手段包括以倍频、和频和光参量振荡器 (OPO) 等为代表的二阶非线性效应[54−57], 以及受激拉曼散射 (SRS) 和受激布里渊散射 (SBS) 等为代表的三阶非线性效应[58−61]。对比二阶非线性效应, SRS 和 SBS 不受相位匹配条件的限制, 因此只要工作波长在材料的透明区域并达到激发阈值即可工作, 结合 SRS 和 SBS 固有的级联频率转换特性, 拉曼和布里渊激光器能够在一个增益介质中产生若干频率的 Stokes 光输出[60,62−65]。同时, SRS 和 SBS 固有的相位共轭特性使其能够实现高亮度高光束质量的输出[66−68]。此外, SRS 的频移量通常比 SBS 高两三个数量级 (以晶体材料为例), 即拉曼激光器的波长跨度范围大, 因此, 基于 SRS 的拉曼激光器通过光学镀膜即可实现对不同波长激光参数的增益和损耗控制。综上, 拉曼激光器在实现多波长激光方面具有显著的优势, 其中基于晶体拉曼转换的多波长激光器以其结构紧凑、性能稳定等优点成为人们关注的重点。

文中介绍了拉曼激光器的工作原理, 归纳了自由空间拉曼振荡器的常见结构和典型的拉曼晶体特性, 综述了基于晶体拉曼转换的多波长激光技术发展现状, 拟通过该文为开展多波长激光技术研究和应用的人员提供有价值的参考。

## 1 拉曼激光器的基本原理

### 1.1 SRS 原理

当以高强度的相干激光入射拉曼增益介质时, 激发增益介质内部分子的振动, 导致相干光被散射的同时产生受激光学声子 (SBS 产生的为声学声子), 受激光学声子将继续参与相干散射过程并极速增加所形成的一种雪崩过程, 在该过程中产生的具有相同频率的相干散射光即为 SRS, 其过程如图 2 所示[69−71]。

SRS 作为一种非弹性弹射也可实现从一阶到级联的频率变换, 即当一束光入射拉曼增益介质并达到激发阈值时, 首先会产生与入射光存在一定频率差的 Stokes 光, 即一阶 Stokes 光; 当一阶 Stokes 光功率密度不断增加并达到下一阶阈值时, 会激发二阶 Stokes 光; 以此类推, 随着功率密度不断上升, 可逐级形成三阶、四阶乃至更高阶次的 Stokes 光, 在此过程中通常低阶的 Stokes 光会维持稳态。级联 SRS 过程示意图如图 3 所示[35,71], 对于拉曼转换, 其频率满足 $\omega_{s1}$=

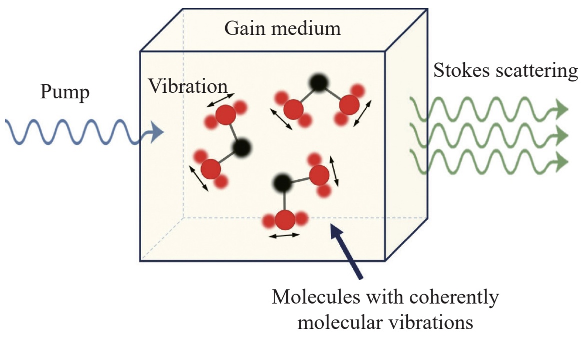


图 2 SRS 激发过程示意图

Fig.2 Schematic diagram of SRS excitation process

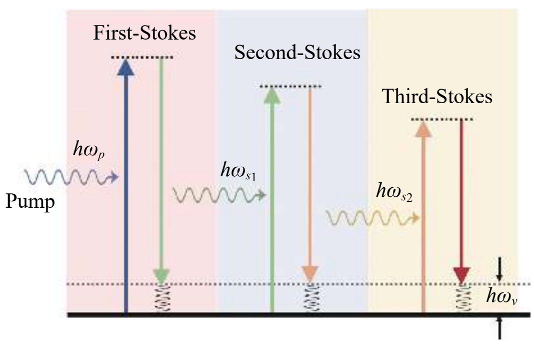


图 3 级联受激拉曼散射过程示意图

Fig.3 Schematic diagram of the cascaded SRS process

$\omega_p-\omega_v$，其中 $\omega_{s1}$、$\omega_p$、$\omega_v$ 分别为一阶 Stokes 光、泵浦光和分子振动的频率。因此，利用谐振腔所造成的光能量损耗设计输入/输出镜对各个阶次光的反射率，可实现多阶次 Stokes 光即多波长激光输出，即二阶 Stokes 光为 $\omega_{s2}=\omega_{s1}-\omega_v$，三阶 Stokes 光为 $\omega_{s3}=\omega_{s2}-\omega_v$。

### 1.2 拉曼激光器的结构

拉曼激光器的输出波长是由泵浦光波长和拉曼增益介质的固有频移决定的，即在拉曼增益介质的透过光谱范围内，通过改变泵浦波长即可获得不同波长的一阶拉曼光输出，进而可以结合级联 SRS 实现多波长输出。但是，受限于拉曼增益介质有限的长度，通常需要借助振荡器这一载体实现拉曼激光器的波长选择和转换效率提升。值得一提的是，拉曼激光器中不存在粒子数反转激光器中的“空间烧孔”效应，因此，在波长拓展的同时还可通过优化设计实现窄光谱或单纵模运转[72−75]。

拉曼激光器宏观上可根据激光工作物质与拉曼增益介质是否在同一个振荡器中，分为内腔拉曼激光器和外腔拉曼激光器，而当振荡器中的激光工作物质与拉曼增益介质为相同材料时，通常将其定义为自拉曼激光器[76]。图 4 展示了几种典型的拉曼振荡器结构，由于笔者综述内容主要针对块状的晶体材料，故讨论的结构和研究进展不包含光纤、波导、片上等导波拉曼激光器。

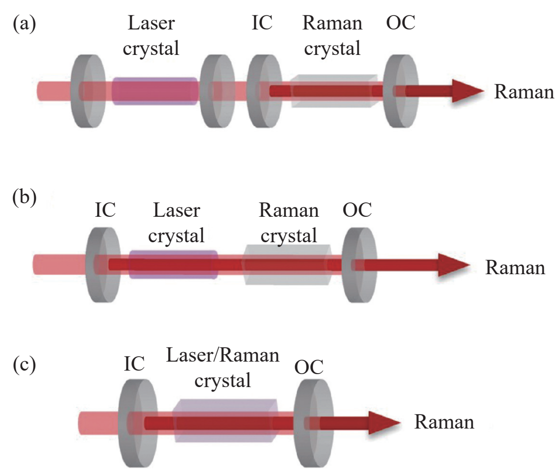


图 4 典型拉曼激光振荡器的结构示意图。(a) 外腔型；(b) 内腔型；(c) 自拉曼

Fig.4 Schematic diagram of typical Raman lasr oscillator structure. (a) External cavity; (b) Intracavity; (c) Self-Raman

图 4(a) 为外腔型拉曼激光器的结构示意图，该结构中的激光工作物质与拉曼增益介质均独立成腔，其优点是拉曼振荡器的泵浦光不受激光振荡器的制约，无论在拉曼增益介质选择、腔型结构设计还是系统热管理方面都更加灵活，且输出参数可控性强。图 4(b) 为内腔型拉曼激光器的结构示意图，激光晶体与拉曼晶体介质放置在同一个振荡器内，该结构的特点在于腔内的高功率密度有助于拉曼增益介质充分利用泵浦功率，因此相对于外腔拉曼振荡器具有更高的拉曼转换效率，且结构紧凑。但是内腔型拉曼也面临着结构设计复杂、振荡器腔镜镀膜难度高、系统热管理复杂等问题。图 4(c) 为自拉曼激光器的结构示意图，该结构中的材料需要兼具激光工作物质与拉曼增益介质的功能，因此需要具有较高的拉曼增益系数，常见的自拉曼晶体材料包括 $Nd:YVO_4$、$Nd:GdVO_4$ 等。该结构的特点在于可大幅缩短腔长、结构更加紧凑，但是也面临着材料热负载严重、输出功率不高、输出参数单一且难以控制的瓶颈。

### 1.3 典型的晶体拉曼增益介质

目前,人们利用气态、液态和固态介质均已实现拉曼激光运转。气态拉曼介质往往是分子型活性材料,常见有氢气 ($H_2$)、氧气 ($O_2$)、氮气 ($N_2$)、甲烷 ($CH_4$) 和二氧化碳 ($CO_2$) 等气体[77−81]。气态拉曼介质具有拉曼频移高、透过谱宽、光学均匀性好且成本低等特点。但是,气体的使用存储过程往往需要高压密闭装置且介质热导率通常较低。常见的液态受激拉曼介质有苯、乙醇、水、二硫化碳等[82−85]。液态拉曼介质具有拉曼增益较高、抗光损伤阈值高、拉曼频移丰富、光谱宽等特点。但是,液态拉曼介质往往也存在挥发性、部分有毒性、分子不稳定等固有缺陷。固态拉曼介质目前应用较为广泛,近年来拉曼晶体介质展现出散热性好、透过光谱宽、热导率高、拉曼增益高等优点,因此,越来越多基于拉曼晶体的激光器被研发与应用[61]。目前,常用的拉曼晶体介质包括金刚石[86−88]、硝酸盐[89−90]、钨酸盐[91−95]、钒酸盐[96−98] 等。表 1 列出了几种典型固体拉曼晶体介质及其特性。相较于气态/液态介质,拉曼晶体不仅具有拉曼频移量大、热导率高、输出光束质量良好等显著优势,而且拉曼晶体中高度对称排列的原子和分子使得拉曼晶体抑制谱线加宽能力强,抗干扰能力强。

**表 1 室温下典型拉曼晶体特性**

**Tab.1 Properties of typical Raman crystals at room temperature**

| Material | Frequency shift/ $cm^{-1}$ | Raman gain coefficient/ $cm\cdot GW^{-1}$ | Thermal conductivity/ $W\cdot m^{-1}\cdot K^{-1}$ | Thermal expansion/ $\times 10^{-6}\ K^{-1}$ | Transmission range/ μm |
|---|---|---|---|---|---|
| Diamond | 1 332.3 | ~15 | 2 000 | 1.1 | >0.23 |
| $Ba(NO_3)_2$ | 1 047.3 | 11 | 1.17 | 13 | 0.35-1.8 |
| $BaWO_4$ | 924/332 | 8.5 | 3 | - | 0.25-5.1 |
| $SrWO_4$ | 921 | 5.0 | 2.9 | - | 0.3-2.7 |
| KGW | 89/901/768 | 3.5 | 2.6 | 4.0 | 0.34-5.5 |
| $YVO_4$ | 259/376/816/838/890 | 4.5 | 5.2 | 4.43 | 0.4-5.0 |
| $GdVO_4$ | 885 | 4.5 | 10.5 | 1.5 | 0.35-5.0 |
| $LiIO_3$ | 822/770 | 4.8 | 4 | 28 | 0.31-4.0 |
| $KY(WO_4)_2$ | 905/765 | 3.6 | 3.3 | 1.83 | 0.35-5.5 |
| Silicon | 521 | - | 153 | 3 | >1.1 |

## 2 基于晶体拉曼转换的多波长激光技术发展现状

综上,根据激光工作物质与拉曼增益介质的相对位置不同将拉曼激光器分为内腔、外腔和自拉曼激光器三种。为了更好地实现其细分,文中结合具体的空间腔型结构将多波长拉曼激光器分为线形腔、环型和折叠型腔、微型腔三类,并对其发展现状进行总结。

### 2.1 线形腔结构

线形腔结构是最常见的一种实现多波长输出的谐振腔型,其特点在于引入的光学元件少,腔内等效热效应处理难度低,有利于提高输出光功率及光-光转换效率和实现小型化。

2012 年,山东大学 Shen H.等人[99] 利用 $BaWO_4$ 晶体作为拉曼增益介质,通过激光二极管 (LD) 侧面泵浦声光调 $Q$ 的内腔拉曼振荡器结构,实现了一阶 1 180 nm 和二阶 1325 nm 的双波长级联拉曼输出,在重复频率为 15 kHz 时,获得了双波长最大输出功率分别为 8.30 W 和 2.84 W、脉冲宽度分别为 20.5 ns 和 5.8 ns,作者在实验中观察到了锁模脉冲,实验装置见图 5。2012 年,江苏师范大学的 Huang H.等人[100] 利用 KTP 晶体与 KTA 晶体作为拉曼增益介质,基于 LD 端面泵浦 $Nd:YAG/Cr^{4+}:YAG$ 键合晶体的内腔拉曼振荡器,实现了 1 091 nm 和 1 095 nm 正交偏振双波长输出,对应双波长的最大输出功率分别为 170 mW 和 150 mW,脉冲宽度为 3.3 ns,重复频率为 11.2 kHz。2014 年,山东大学的 Zhang H.等人[101] 实现了 LD 端面泵浦主动调 $Q$ 的 $Nd:YAG/BaWO_4$ 内腔拉曼激光器的双波长输出,一阶 Stokes 光和二阶 Stokes 光的波长分别为 1 240 nm 和 1 376 nm,重复频率为 10 kHz 时获得的最

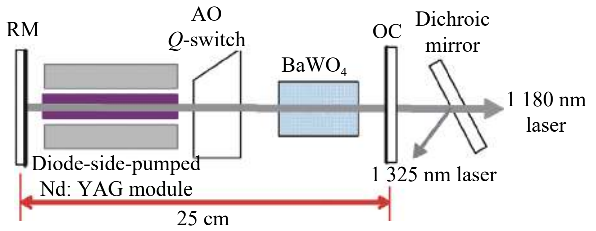


图 5 多波长 $BaWO_4$ 拉曼激光器示意图[99]

Fig.5 Schematic diagram of a multi-wavelength Raman laser in $BaWO_4$ [99]

大输出功率分别为 869 mW 和 512 mW。2015 年，台湾交通大学 Huang H.J.等人[102] 利用 KTP 和 KTA 晶体作为拉曼增益介质，基于 LD 端面泵浦 Nd:YAP 的声光调 $Q$ 内腔拉曼振荡器结构，分别实现了 1478 nm 和 1 503 nm 双波长，以及 1474 nm 和 1480 nm 的双波长人眼安全激光输出。2016 年，中国科学院大学的 Sun Y.等人[103] 用 KGW 晶体中 768 $cm^{-1}$ 和 901 $cm^{-1}$ 的两个正交偏振拉曼偏移，经旋转 Yb:GAB 激光晶体 90°分别实现 1 133.1、1 156.6 nm 和 1 137.8、1 151.9 nm 的正交偏振双波长输出。2020年，暨南大学 Tu Z.等人[104] 基于主动调 $Q$ 的 Nd:YLF/KGW 的内腔拉曼振荡器结构，经旋转 KGW 晶体 90°分别实现波长 1 470、1 490 nm 和 1 461、1 499 nm的正交偏振双波长激光输出。2020 年，温州大学的 Duan Y.等人[105] 报道了一台声光调 $Q$ 的 $Nd:YAP/YVO_4$ 级联拉曼激光器，结合 BBO 晶体角度调谐，实现了 539.9、567.2、597.4、631.0、668.5 nm 五种波长的激光输出，该方案为实现多波长可切换激光输出提供了一种新思路。2020 年，扬州大学樊莉等人[106] 设计了一款 $Nd:YVO_4/BaWO_4$ 连续波多波长拉曼激光器，利用 $BaWO_4$ 晶体中的 925 $cm^{-1}$ 和 332 $cm^{-1}$ 的频移量和 $YVO_4$ 晶体中的 890 $cm^{-1}$ 频移，获得 1 103.6 nm、1 175.9 nm 和 1 180.7 nm 的三个一阶 Stokes 光和 1 145.7 nm 和 1 228.9 nm 的两个二阶 Stokes 光的输出。

金刚石作为一种具有超高热导率和极宽光谱透过范围的拉曼晶体，在实现高功率多波长激光输出方面具有显著优势[107−110]。2014 年，澳大利亚麦考瑞大学 McKay A.等人[111] 利用纳秒脉冲泵浦外腔金刚石拉曼振荡器，在 36.5 kHz 脉冲重复频率泵浦时产生总功率 14.5 W 的 1 240 nm 一阶和 1 485 nm 二阶拉曼激光输出。2021 年，河北工业大学的白振旭等人[24] 报道了一台可实现 1.2 μm 和 1.5 μm 双波长输出的百瓦级外腔金刚石拉曼激光器，1.2 μm 和 1.5 μm 的稳态功率分别为 72 W 和 110 W，且输出的光谱相对于泵浦光的均出现一定的窄化，实验装置如图 6 所示。近期，该团队研制了一台 532 nm 绿光泵浦的多波长级联金刚石拉曼激光器，通过将一阶 Stokes 黄橙光 (573 nm) 锁定在振荡器中，实现了 620 nm、676 nm 和 743 nm 的级联拉曼激光输出，对应三个波长的脉冲宽度分别为 10.41 ns、3.75 ns 和 2.45 ns，总峰值功率为 70.7 kW。

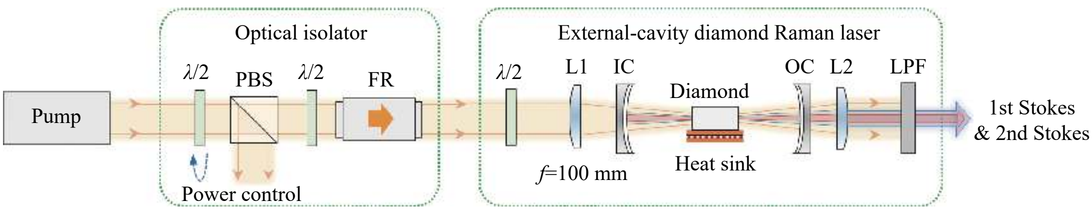


图 6 百瓦级金刚石拉曼激光器示意图[24]

Fig.6 Schematic diagram of a hundred-watt diamond Raman laser[24]

## 2.2 非线形腔结构 (环形腔和折叠腔)

非线形腔结构主要包括环形腔和折叠腔两种，此类腔型由三个及以上的腔镜组成，其区别在于折叠腔与线形腔均为驻波腔，而环形腔内的光束为行波传输。环形腔的特点是易于实现光束的单向传播，且便于形成腔增强结构以提高振荡器内的功率密度[112−114]；折叠腔典型结构包括“V”字型、“Z”字型腔等，其相比于线形腔具有腔内模式设计灵活、易于进行双端泵浦等[115−117]。

2014 年，澳大利亚麦考瑞大学的 Warrier A.M.等[118] 报道了一台同步泵浦的 1 240 nm 和 1 485 nm 皮秒金刚石拉曼激光器，实现了 1 240 nm 一阶 Stokes 光功率 2.75 W 的输出，并通过结合四波混频和单通 SRS 获得了 1485 nm 的二阶 Stokes 光功率为 1.0 W 的

输出。2020 年,麦考瑞大学的 Li M.等人[119] 报道了一台可调谐钛宝石连续波激光器谐振泵浦的金刚石拉曼环形腔激光器,获得了波长为 964.9 nm 的一阶 Stokes 光和 1101.3 nm 的二阶 Stokes 光,并实现了单纵模的运转,实验装置如图 7 所示。随后,笔者利用数学模型表征了高阶 Stokes 系统的损耗和斜效率,提出二阶 Stokes 光输出功率可通过改进光束的传播方向来优化[120]。2021 年,捷克布拉格技术大学的 Frank M.等人[121] 利用混合掺杂的 $Pb(MoO_4)_{0.2}(WO_4)_{0.8}$ 作为拉曼晶体,结合环型谐振腔结构,实现了在 1128~1360 nm 光谱范围内的 12 个短波长间隔的激光输出,并提出优化拉曼晶体的掺杂,腔镜的反射率有望提高多波长转换效率。

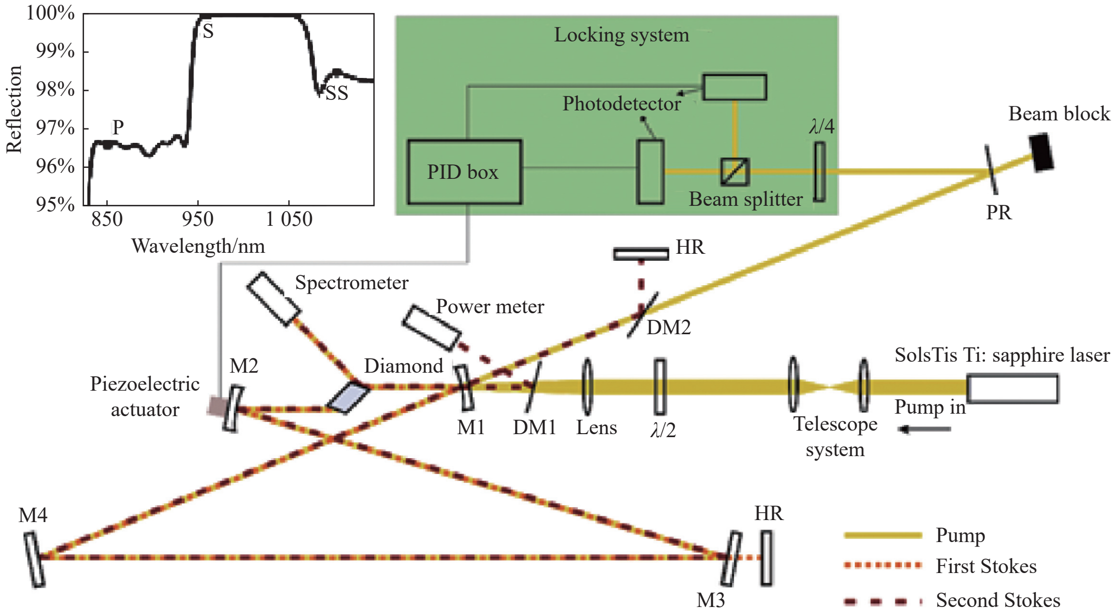


图 7 金刚石拉曼激光器示意图,插图为 IC/OC 的光谱图[119]

Fig.7 Schematic diagram of diamond Raman laser, illustrated with IC/OC spectrogram[119]

2010 年,麦考瑞大学的 Eduardo G.等人[122] 报道了一台级联连续波锁模 KGW 拉曼振荡器,利用脉冲宽度为 28 ps 的 532 nm 激光作为泵浦源,基于"Z"型腔结构,实现了一阶 559 nm 和二阶 589 nm 的拉曼转换输出,对应脉冲宽度为 6.5 ps 和 5.5 ps,功率分别为 2.5 W 和 1.4 W。2011 年,英国思克莱德大学 Parrotta D. C.等人[123] 利用 LD 泵浦 InGaAs 的半导体圆盘激光器为金刚石拉曼激光器提供泵浦,实现了波长 1217~1244 nm 范围内的可调输出,其中波长 1227 nm 时的一阶 Stokes 光输出功率为 1.3 W。虽然该研究并非真正意义的多波长拉曼激光器,但是作者验证了基于晶体拉曼实现连续可调波长变换的可行性,对后续折叠腔实现多波长激光具有一定的参考意义,后续国内外多个团队围绕波长可调的晶体拉曼激光器开展了相关研究工作[74,87,124]。在 2018 年,英国思克莱德大学同一团队的 Casula R.等人[125] 研制了一台基于 KGW 晶体的多波长拉曼激光器,通过旋转放置在谐振腔内的双折射滤光片,最终实现 1.32、1.50、1.73 μm 的三波长级联 Stokes 光输出,每个波长功率均实现了瓦级输出,实验装置如图 8 所示。

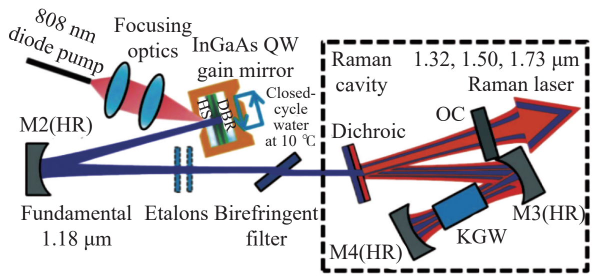


图 8 基于 KGW 的多波长级联拉曼激光器示意图[125]

Fig.8 Schematic diagram of the cascaded Raman laser in KGW[125]

### 2.3 微腔结构

微型谐振腔结构是由不同透过率的输入/输出耦合镜直接与晶体紧密接触形成的激光器结构。微型

谐振腔多波长激光器具有腔长短、易于实现短脉冲等优点。由于参与键合的晶体往往需要是相同或相近的基质，因此目前基于微腔的多波长拉曼激光器主要是利用 $YVO_4$ 晶体与激光晶体键合。

2016 年，厦门大学 Wang X. L.等人[35] 报道一台 LD 泵浦 Yb:YAG/Nd:$YVO_4$ 多波长连续波微片拉曼激光器，采用 a 切 Nd:$YVO_4$ 晶体作为拉曼转换介质，实现了 1.05 μm 和 1.08 μm 的双波长激光输出。2018 年，该团队[126] 利用 Nd:$GdVO_4$/$Cr^{4+}$:YAG/ $YVO_4$ 拉曼微片激光器实现了 1 164.4 nm 和 1 174.7 nm 的同步脉冲双波长输出，双波长激光脉冲宽度为 825 ps、峰值功率超过 1 kW，实验装置如图 9 所示。

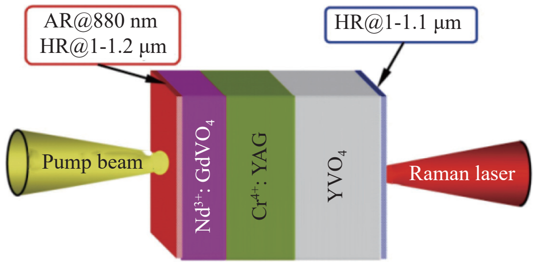


图 9 Nd:$GdVO_4$/$Cr^{4+}$:YAG/$YVO_4$ 微片激光器[126]

Fig.9 Schematic diagram of a Nd:$GdVO_4$/$Cr^{4+}$:YAG/$YVO_4$ microchip laser[126]

### 2.4 小 结

表 2 总结了基于拉曼转换多波长激光器的参数。结合研究现状不难发现，线形腔仍是目前最常用的产

表 2 多波长拉曼激光器研究现状

**Tab.2 Research status of multi-wavelength Raman laser**

| Year | Cavity type | Cavity structure | Pumping method | Pump wavelength | Raman crystal | Output wavelength | Output power | Ref. |
|---|---|---|---|---|---|---|---|---|
| 2012 | Intracavity | Linear cavity | Pulsed | 808 nm | $BaWO_4$ | 1 180 nm<br>1 325 nm | 8.30 W<br>2.84 W | [99] |
| 2012 | Intracavity | Linear cavity | Pulsed | 808 nm | KTP/KTA | 1 091 nm<br>1 095 nm | 170 mW<br>150 mW | [100] |
| 2014 | Intracavity | Linear cavity | Pulsed | 808 nm | $BaWO_4$ | 1 240 nm<br>1 376 nm | 869 mW<br>512 mW | [101] |
| 2014 | External cavity | Linear cavity | Pulsed | 1 064 nm | Diamond | 1 240+1 485 nm | 14.5 W | [111] |
| 2015 | Intracavity | Linear cavity | Pulsed | 808 nm | KTP/KTA | 1 478 nm<br>1 503 nm | 117 mW<br>389 mW | [102] |
| 2016 | Intracavity | Linear cavity | Pulsed | 976 nm | KGW | 1 133+1 156 nm<br>1 137+1 151 nm | 155 mW<br>154 mW | [103] |
| 2020 | Intracavity | Linear cavity | Pulsed | 808 nm | KGW | 1 470+1 490 nm<br>1 461+1 499 nm | 2.6 W<br>2.4 W | [104] |
| 2020 | Intracavity | Linear cavity | Pulsed | 804 nm | $YVO_4$ | 539.9+567.2+597.4+<br>631.0+668.5 nm | 800,340,460,<br>190,326 mW | [105] |
| 2020 | Intracavity | Linear cavity | CW | 879 nm | $BaWO_4$+$YVO_4$ | 1 103.6+1 175.9+1 180.7+<br>1 145.7 +1 228.9 nm | 1.24 W<br>(MAX) | [106] |
| 2021 | External cavity | Linear cavity | QCW | 1 064 nm | Diamond | 1 240 nm<br>1 485 nm | 72 W<br>110 W | [24] |
| 2023 | External cavity | Linear cavity | Pulsed | 532 nm | Diamond | 620 nm<br>676 nm<br>743 nm | 12.5 kW*<br>40.8 kW*<br>17.4 kW* | |
| 2010 | External cavity | Z-fold | CW | 1 064 nm | KGW | 559 nm<br>589 nm | 2.5 W<br>1.4 W | [122] |
| 2014 | External cavity | Ring-cavity | Pulsed | 1 064 nm | Diamond | 1 240 nm<br>1 485 nm | 2.75 W<br>1.0 W | [118] |
| 2020 | External cavity | Ring-cavity | CW | 845-930 nm | Diamond | 965 nm<br>1 101 nm | 400 mW<br>364 mW | [119] |
| 2021 | External cavity | Ring-cavity | Pulsed | 1 063 nm | $Pb(MoO_4)_{0.2}(WO_4)_{0.8}$ | 1 128 nm<br>1 360 nm | watt level | [121] |
| 2018 | External cavity | Z-fold | CW | 808 nm | KGW | 1.32 μm<br>1.50 μm<br>1.73 μm | 6.1 W<br>1.1 W<br>1.1 W | [125] |
| 2016 | Intracavity | Microcavity | CW | 808 nm | Nd:$YVO_4$ | 1.05 μm<br>1.08 μm | 260 mW | [35] |
| 2019 | Intracavity | Microcavity | Pulsed | 880 nm | $YVO_4$ | 1 164 nm<br>1 175 nm | 40 mW | [126] |

*Peak power

生多波长拉曼激光的谐振腔结构,且围绕脉冲激光的研究占比最高;相比于内腔拉曼振荡器,外腔拉曼振荡器的平均和峰值功率更高,展现了更为强大的功率拓展性;微腔拉曼激光器目前输出功率与转换效率均较低,但其具有高重复频率与小型化等特点。

## 3 结 论

文中简述了 SRS 的工作原理、拉曼振荡器的基本结构以及拉曼晶体的特性,对基于晶体拉曼转换的多波长激光的研究现状进行了综述。虽然围绕晶体拉曼转换的多波长激光器的研究仅有十余年,但是诸多新晶体、新结构和新波长不断被探索,尤其近年来随着金刚石晶体等新晶体材料趋于成熟,使多波长拉曼激光器在功率提升、波长拓展和小型化等方面有着不凡的表现。笔者认为,为了全面提升多波长拉曼激光器的性能,今后的研究将主要围绕以下方面展开,即:优化泵浦光参数和优化振荡器设计提高转换效率,避免级联阶次的增加导致的量子效率降低;拓展多波长激光的输出光谱范围,实现波长和波段的参数可控输出;高功率运转下的热管理,提高系统的稳定性和光束质量;与结构光产生技术相结合,拓展多波长激光器的维度。未来,基于晶体介质的拉曼激光器有望成为多波长激光产生和应用的主力军。

**参考文献:**

[1] Chellappan K V, Erden E, Urey H. Laser-based displays: a review [J]. ***Applied Optics***, 2010, 49(25): F79-F98.

[2] Bai Z, Chen H, Gao X, et al. Highly compact nanosecond laser for space debris tracking [J]. ***Optical Materials***, 2019, 98: 109470.

[3] Chen Hui, Bai Zhenxu, Wang Jiancai, et al. Hundred-watt green picosecond laser based on LBO frequency-doubled photonic crystal fiber amplifier [J]. ***Infrared and Laser Engineering***, 2021, 50(11): 20200522. (in Chinese)

[4] Sun Sijia, Tian Wenlong, Yang Yunxiao, et al. Visible rare-earth doped solid-state lasers (*invited*) [J]. ***Electro-Optic Technology Application***, 2023, 38(1): 11-20. (in Chinese)

[5] Yu J, Luo M, Lv Z, et al. Recent advances in optical and optoelectronic data storage based on luminescent nanomaterials [J]. ***Nanoscale***, 2020, 12(46): 23391-23423.

[6] Lin X, Wang P, Zhang Y, et al. Theoretical and experimental aspects of laser cutting using direct diode laser source based on multi-wavelength multiplexing [J]. ***Optics Laser Technology***, 2019, 114: 66-71.

[7] Ding Yu, Jiang Feng, Zheng Rongshan, et al. Overview of high energy laser weapon development in USA (*invited*) [J]. ***Electro-Optic Technology Application***, 2021, 36(6): 1-9. (in Chinese)

[8] Khalkhal E, Rezaei-tavirani M, Zali Mr, et al. The evaluation of laser application in surgery: A review article [J]. ***Journal of Lasers in Medical Sciences***, 2018, 10(Suppl1): S104-S111.

[9] Gu Yonggang, Niu Jian, Yang Jian, et al. Application of laser in the medical field [J]. ***Chinese Optics***, 2023, 16(2): 283-295. (in Chinese)

[10] Long Mingliang, Deng Huarong, Zhang Haifeng, et al. Pulse burst picosecond laser technique and application in space debris ranging [J]. ***Electro-Optic Technology Application***, 2022, 28(6): 45-52. (in Chinese)

[11] Sijan A. Development of military lasers for optical countermeasures in the mid-IR[C]//Proceedings of SPIE, 2009, 7483: 748304.

[12] Li S, Yan X. Research on mid-infrared laser source in laser countermeasure system and key technology [J]. ***Electro-Optic Technology Application***, 2018, 33(5): 19-23. (in Chinese)

[13] Li Chunguang, Dang Jingmin, Chen Chen, et al. Multi-Pass absorption spectroscopy for CO detection using a quantum cascaded laser [J]. ***Spectroscopy and Spectral Analysis***, 2016, 36(5): 1308-1312. (in Chinese)

[14] Bai Zhenxu, Gao Jia, Zhao Chen, et al. Research progress of long-wave infrared lasers based on nonlinear frequency conversion [J]. ***Acta Optica Sinica***, 2023, 43(3): 0314001. (in Chinese)

[15] Wang C C, Liu R K, Wang T Y, et al. Applications of infrared semiconductor laser [J]. ***Laser Journal***, 2020, 41(8): 1-10. (in Chinese)

[16] Gebbie H A, Harding W R, Hilsum C, et al. Atmospheric transmission in the 1 to 14 μ region [J]. ***Proceedings of the Royal Society A: Mathematical and Physical Sciences***, 1951, 206(1084): 87-107.

[17] Liu Yuqing, Sun Hongbo. Progress and application of nonlinear laser manufacturing (*invited*) [J]. ***Infrared and Laser Engineering***, 2022, 51(1): 20220005. (in Chinese)

[18] Tunna L, Kearns A, O'neill W, et al. Micromachining of copper

using Nd: YAG laser radiation at 1 064, 532, and 355 nm wavelengths [J]. ***Optics & Laser Technology***, 2001, 33(3): 135-143.

[19] Huo X, Qi Y, Zhang Y, et al. Research development of 589 nm laser for sodium laser guide stars [J]. ***Optics and Lasers in Engineering***, 2020, 134: 106207.

[20] You Wei, Yang Xuezong, Chen Weibiao, et al. Review of 589 nm sodium laser guide stars (*invited*) [J]. ***Electro-Optic Technology Application***, 2021, 36(5): 1-14,32. (in Chinese)

[21] Rauter P, Capasso F. Multi - wavelength quantum cascade laser arrays [J]. ***Laser & Photonics Reviews***, 2015, 9(5): 452-477.

[22] Zhang Xiaolin, Zhu Li, Huang Bo, et al. Effect of multi-wavelength laser on nerve fiber layer in patients with DR and possible mechanisms [J]. ***Chin J Laser Med Surg***, 2020, 29(6): 336-341. (in Chinese)

[23] Liu Chenkai, Hu Mingyong, Li Zhaoyang, et al. Design of a multi-wavelength lidar optical system [J]. ***Chinese Journal of Quantum Electronics***, 2021, 38(6): 806-814. (in Chinese)

[24] Bai Zhenxu, Chen Hui, Zhang Zhanpeng, et al. Hundred-watt dual-wavelength diamond Raman laser at 1.2 /1.5 µm (*invited*) [J]. ***Infrared and Laser Engineering***, 2021, 50(12): 20210685. (in Chinese)

[25] Marshall J, Stewart G, Whitenett G. Design of a tunable L-band multi-wavelength laser system for application to gas spectroscopy [J]. ***Measurement Science and Technology***, 2006, 17(5): 1023.

[26] Bai Zhenxu, Chen Hui, Ding Jie, et al. High-power brillouin frequency comb based on free-space optical cavity [J]. ***Chinese Journal of Lasers***, 2022, 49(4): 0415001. (in Chinese)

[27] Photogrammetry vs. LIDAR: what sensor to choose for a given application[EB/OL]. (2023-01-27)[2023-07-06]. https://wingtra.com/drone-photogrammetry-vs-lidar/.

[28] Photonics Applied: Ddfense: IR countermeasures aim for safer [EB/OL]. (2021-08-01) [2023-07-06]. https://www.laserfocusworld.com/lasers-sources/article/16548073/photonics-applied-defense-ir-countermeasures-aim-for-safer-flights.

[29] High speed laser communication is now available in space [EB/OL]. (2016-02-06)[2023-07-06]. https://incompliancemag.com/high-speed-laser-communication-in-space/.

[30] Zapping away: medical laser systems are winning big in the modern hospital[EB/OL]. (2017-08-08)[2023-07-06]. https://blog.technavio.org/blog/medical-laser-technologies-market.

[31] Laser-scanning microscopy method achieves rapid 3D imaging[EB/OL]. (2022-03-21)[2023-07-06]. https://www.photonics.com/Articles/Laser-Scanning_Microscopy_Method_Achieves_Rapid/a67871.

[32] Chen L, Wen X, Zhang H, et al. Different wavelength krypton lasers in treatment of diabetic retinopathy [J]. ***Chin J Ocul Fundus Dis***, 2001, 17(3): 178-180. (in Chinese)

[33] Wang Zhen. Study on multi-wavelength fiber lasers with narrow line width and their applications[D]. Changchun: Changchun University of Science and Technology, 2018. (in Chinese)

[34] Deng Yuxiang. Multiwavelength Brillouin erbium-doped fiber laser with wavelength spacing of multiple Brillouin shift[D]. Nanjing: Nanjing University of Posts and Telecommunications, 2018. (in Chinese)

[35] Wang X L, Dong J, Wang X J, et al. Multi-wavelength Yb: YAG/$Nd^{3+}$: $YVO_4$ continuous-wave microchip Raman laser [J]. ***Opt Lett***, 2016, 41(15): 3559-3562.

[36] Sun S, Wei Q, Li B, et al. The $YMgB_5O_{10}$ crystal preparation and attractive multi-wavelength emission characteristics of doping $Nd^{3+}$ ions [J]. ***Journal of Materials Chemistry C***, 2021, 9(6): 1945-1957.

[37] Chen Longhui, Xie Fang, Guo Xiaolei, et al. Research on tunable single-longitudinal multi-wavelength fiber laser [J]. ***Laser Technology***, 2021, 45(6): 681-685. (in Chinese)

[38] Liu Hao, Shu Rong, Hong Guanglie, et al. Continuous-wave modulation differential absorption lidar system for $CO_2$ measurement [J]. ***Acta Phys Sin***, 2014, 63(10): 104214.

[39] Shi Yile. Research on practical approach of color computer-generated rainbow holography[D]. Suzhou: Soochow University, 2013. (in Chinese)

[40] Kang Peng, Sun Yu, Wang Jin, et al. Measurement of molecular absorption spectrum with a laser locked on a high-finesse cavity [J]. ***Acta Phys Sin***, 2018, 67(10): 104206. (in Chinese)

[41] Zhong Kai, Zhang Xianzhong, Xu Degang, et al. Progress of all-solid-state dual-wavelength lasers (*invited*) [J]. ***Electro-Optic Technology Application***, 2022, 37(4): 13-26, 78. (in Chinese)

[42] Xia J, Lv Y, Liu H, et al. Diode-pumped $Pr^{3+}$: $LiYF_4$ visible dual-wavelength laser [J]. ***Optics Communications***, 2015, 334: 160-163.

[43] Wang Yongheng, Zhao Changming, Cai Zitao, et al. LD pumped 1 061 nm/1 064 nm dual-wavelength Nd: YAG micro-chip laser [J]. ***Chinese Journal of Lasers***, 2020, 47(3): 0301002. (in Chinese)

[44] Chen Lijuan, Wang Zhengping, Zhuang Shidong, et al. Dual-wavelength Nd: YAG crystal laser at 1 074 and 1 112 nm [J]. ***Opt Lett***, 2011, 36(13): 2554.

[45] Jia Fuqiang, Xue Qinghua, Zheng Quan, et al. All-solid-state 556-nm yellow laser by LBO intracavity-frequency-doubling [J]. ***Chinese Journal of Lasers***, 2005, 32(8): 1017-1021. (in Chinese)

[46] Zhang X, Zhang S, Wang C, et al. Orthogonally polarized dual-wavelength single-longitudinal-mode Tm, Ho: LLF laser [J]. ***Optics Express***, 2013, 21(19): 22699-22704.

[47] Cui Can, Wang Yue, Wang Yulei, et al. Research progress on nonlinear optics laser beam combining technology [J]. ***High Power Laser and Particle Beams***, 2023, 35: 041006. (in Chinese)

[48] Bai Zhenxu, Wang Yulei, Lv Zhiwei, et al. Research progress of serial laser beam combination based on stimulated Brillouin amplification [J]. ***Laser & Optoelectronics Progress***, 2015, 52(11): 110004. (in Chinese)

[49] Zhou Pu, Su Rongtao, Ma Yanxing, et al. Review of coherent laser beam combining research progress in the past decade [J]. ***Chinese Journal of Lasers***, 2021, 48(4): 0401003. (in Chinese)

[50] Liu Xiaoxi, Wang Xuefeng, Wang Junlong, et al. External cavity spectral beam combining of fiber lasers [J]. ***Chinese Journal of Lasers***, 2018, 45(8): 0801009. (in Chinese)

[51] Zhang D, Hao J, Zhu C, et al. Review on spectral beam combining of fiber lasers [J]. ***Laser & Infrared***, 2016, 46(5): 517-521. (in Chinese)

[52] Zhang Y, Hu M, Xu M, et al. Experimental investigation on the Y-type cavity tunable dual-wavelength laser based on neodymium-doped vanadate crystals [J]. ***Optics Communications***, 2021, 495: 127089.

[53] Fan T Y. Laser beam combining for high-power, high-radiance sources [J]. ***IEEE Journal of Selected Topics in Quantum Electronics***, 2005, 11(3): 567-577.

[54] Sang Mei, Xue Ting, Yu Jian, et al. The characteristics of optical parametrical oscillator in periodically poled KTiOPO [J]. ***Acta Photonica Sinica***, 2003, 32(11): 1286-1290. (in Chinese)

[55] Borsutzky A, Brünger R, Huang C, et al. Harmonic and sum-frequency generation of pulsed laser radiation in BBO, LBO, and KD*P [J]. ***Applied Physics B***, 1991, 52(1): 55-62.

[56] Tan Tianya, Shao Jianda, Fan Zhengxiu, et al. Study on preparation and performances of 1 064 nm, 532 nm frequency-doubled antireflection coating for LBO [J]. ***Acta Optica Sinica***, 2009, 29(7): 2022-2025. (in Chinese)

[57] Shan Pai, Wang Zujian, Su Rongbing, et al. Research progress of quasi-phase matching deep-ultraviolet nonlinear optical crystals [J]. ***Chinese Journal of Quantum Electronics***, 2021, 38(2): 180-184. (in Chinese)

[58] Wu Zhixin. Study on a novel dual-wavelength laser based on stimulated Raman scattering[D]. Jinan: Shandong University, 2019. (in Chinese)

[59] Wang Xiaobin, Kang Wenyun, Song Xiaoquan. Research progress of multi-wavelength laser technology based on Raman crystal [J]. ***Laser & Infrared***, 2016, 46(8): 922-928. (in Chinese)

[60] Bai Z, Yuan H, Liu Z, et al. Stimulated Brillouin scattering materials, experimental design and applications: A review [J]. ***Optical Materials***, 2018, 75: 626-645.

[61] Cheng Mengyao, Duan Yanmin, Sun Yinglu, et al. Research progress of raman and frequency mixing for visible lasers based on vanadate crystals [J]. ***Laser & Optoelectronics Progress***, 2020, 57(7): 071611. (in Chinese)

[62] Chen H, Bai Z, Cai Y, et al. Order controllable enhanced stimulated Brillouin scattering utilizing cascaded diamond Raman conversion [J]. ***Applied Physics Letters***, 2023, 122(9): 092209.

[63] Chen H, Bai Z, Yang X, et al. Enhanced stimulated Brillouin scattering utilizing Raman conversion in diamond [J]. ***Applied Physics Letters***, 2022, 120(18): 181103.

[64] Lin G, Diallo S, Saleh K, et al. Cascaded Brillouin lasing in monolithic barium fluoride whispering gallery mode resonators [J]. ***Applied Physics Letters***, 2014, 105(23): 231103.

[65] Supradeepa V R, Feng Y, Nicholson J W. Raman fiber lasers [J]. ***Journal of Optics***, 2017, 19(2): 023001.

[66] Bai Zhenxu, Chen Hui, Li Yuqi, et al. Development of beam brightness enhancement based on diamond Raman conversion [J]. ***Infrared and Laser Engineering***, 2021, 50(1): 20200098. (in Chinese)

[67] Brauch U, Röcker C, Graf T, et al. High-power, high-brightness

solid-state laser architectures and their characteristics [J]. ***Applied Physics B***, 2022, 128(3): 58.

[68] Gao Q, Lu Z, Zhu C, et al. Mechanism of beam cleanup by stimulated Brillouin scattering in multimode fibers [J]. ***Applied Physics Express***, 2015, 8(5): 052501.

[69] Smith R G. Optical power handling capacity of low loss optical fibers as determined by stimulated Raman and Brillouin scattering [J]. ***Applied Optics***, 1972, 11(11): 2489-2494.

[70] Sirleto L, Ferrara M A. Fiber amplifiers and fiber lasers based on stimulated Raman scattering: a review [J]. ***Micromachines***, 2020, 11(3): 247.

[71] Bai Zhenxu, Hao Xin, Zheng Hao, et al. Research progress on high-power free-space Raman amplification technology (*invited*) [J]. ***Infrared and Laser Engineering***, 2023, 52(8): 20230337. (in Chinese)

[72] Li Muye, Yang Xuezong, Sun Yuxiang, et al. Single-frequency continuous-wave diamond Raman laser (*invited*) [J]. ***Infrared and Laser Engineering***, 2022, 51(6): 20210970. (in Chinese)

[73] Sheng Q, Li R, Lee A J, et al. A single-frequency intracavity Raman laser [J]. ***Optics Express***, 2019, 27(6): 8540-8553.

[74] Yang X, Bai Z, Chen D, et al. Widely-tunable single-frequency diamond Raman laser [J]. ***Optics Express***, 2021, 29(18): 29449-29457.

[75] Lux O, Sarang S, Kitzler O, et al. Intrinsically stable high-power single longitudinal mode laser using spatial hole burning free gain [J]. ***Optica***, 2016, 3(8): 876-881.

[76] Bai Zhenxu. Laser technology and diamond brillouin raman laser brightness enhancement research on high power diamond[D]. Harbin: Harbin Institute of Technology, 2018. (in Chinese)

[77] Nakazato M, Nagai T, Sakai T, et al. Tropospheric ozone differential-absorption lidar using stimulated Raman scattering in carbon dioxide [J]. ***Appl Opt***, 2007, 46(12): 2269-2279.

[78] Everall N J, Partanen J P, Barr J, et al. Threshold measurements of stimulated Raman scattering in gases using picosecond KrF laser pulses [J]. ***Optics Communications***, 1987, 64(4): 393-397.

[79] Sentrayan K, Major L, Bryant H L, et al. Laser wavelength, pressure and temperature dependence on the stimulated raman scattering gain in $H_2$ [J]. ***Spectroscopy Letters***, 1992, 25: 627-637.

[80] Tzortzakis S, Tsaknakis G, Papayannis A, et al. Investigation of the spatial profile of stimulated Raman scattering beams in $D_2$ and $H_2$ gases using a pulsed Nd: YAG laser at 266 nm [J]. ***Applied Physics B***, 2004, 79(1): 71-75.

[81] Pine A S. Self, $N_2$, $O_2$, $H_2$, Ar, and He broadening in the $v^3$ band Q branch of $CH_4$ [J]. ***The Journal of Chemical Physics***, 1992, 97(2): 773-785.

[82] Colles M J. Efficient stimulated Raman scattering from picosecond pulses [J]. ***Optics Communications***, 1969, 1(4): 169-172.

[83] Adrain R S, Arthurs E G, Sibbett W. Tunable picosecond transient stimulated Raman scattering in ethanol [J]. ***Optics Communications***, 1975, 15(2): 290-292.

[84] Du Q, Superfine R, Freysz E, et al. Vibrational spectroscopy of water at the vapor/water interface [J]. ***Phys Rev Lett***, 1993, 70(15): 2313.

[85] Serpengüzel A, Chen G, Chang R K. Stimulated Raman scattering of aqueous droplets containing ions: concentration and size determination [J]. ***Particulate Science and Technology***, 1990, 8(3-4): 179-189.

[86] Kitzler O, Mckay A, Mildren R P. Continuous-wave wavelength conversion for high-power applications using an external cavity diamond Raman laser [J]. ***Opt Lett***, 2012, 37(14): 2790-2792.

[87] Sabella A, Piper J A, Mildren R P. Diamond Raman laser with continuously tunable output from 3.38 to 3.80 μm. [J]. ***Opt Lett***, 2014, 39(13): 4037-4040.

[88] Williams R J, Nold J, Strecker M, et al. Efficient Raman frequency conversion of high-power fiber lasers in diamond [J]. ***Laser Photonics Rev***, 2015, 9(4): 405-411.

[89] Murray J T, Powell R C, Peyghambarian N, et al. Generation of 1.5-μm radiation through intracavity solid-state Raman shifting in $Ba(NO_3)_2$ nonlinear crystals [J]. ***Opt Lett***, 1995, 20(9): 1017.

[90] Takei N, Suzuki S, Kannari F. 20-Hz operation of an eye-safe cascade Raman laser with a $Ba(NO_3)_2$ crystal [J]. ***Applied Physics B Lasers Optics Communications***, 2002, 74: 521-527.

[91] Chen X, Zhang X, Wang Q, et al. Highly efficient diode-pumped actively *Q*-switched Nd: YAG-$SrWO_4$ intracavity Raman laser [J]. ***Opt Lett***, 2008, 33(7): 705-707.

[92] Ding S, Zhang X, Wang Q, et al. Theoretical and experimental research on the multi-frequency Raman converter with $KGd(WO_4)_2$ crystal [J]. ***Opt Express***, 2005, 13(25): 10120-10128.

[93] Fan Y X, Liu Y, Duan Y H, et al. High-efficiency eye-safe intracavity Raman laser at 1531 nm with $SrWO_4$ crystal [J]. ***Applied Physics B***, 2008, 93(2-3): 327.

[94] Kuleshov N V, Lagatsky A A, Podlipensky A V, et al. Pulsed laser operation of Yb-doped $KY(WO_4)_2$ and $KGd(WO_4)_2$ [J]. ***Opt Lett***, 1997, 22(17): 1317-1319.

[95] Matsuse M, Deguchi T, Ohtsuka H, et al. Effect of laser pulsewidth on the generation of multi-color laser emission by stimulated Raman scattering and four-wave Raman mixing in a $KGd(WO_4)_2$ crystal [J]. ***Optics Communications***, 2003, 223(4): 411-416.

[96] Kaminskii A A, Ueda K, Eichler H J, et al. Tetragonal vanadates $YVO_4$ and $GdVO_4$ materials for Raman lasers [J]. ***Optics Communications***, 2001, 94(1-3): 201-206.

[97] SU K W, Chang Y T, Chen Y F. Power scale-up of the diode-pumped actively *Q*-switched Nd: $YVO_4$ Raman laser with an undoped $YVO_4$ crystal as a Raman shifter [J]. ***Applied Physics B***, 2007, 88(1): 47-50.

[98] Xu Yang. The research of multi-wavelenth picosecond stimulated Raman laser[D]. Beijing: Beijing University of Technology, 2014. (in Chinese)

[99] Shen H, Wang Q, Zhang X, et al. 1st-Stokes and 2nd-Stokes dual-wavelength operation and mode-locking modulation in diode-side-pumped Nd:YAG/$BaWO_4$ Raman laser [J]. ***Optics Express***, 2012, 20(16): 17823-17832.

[100] Huang H, Shen D, He J. Simultaneous pulse generation of orthogonally polarized dual-wavelength at 1 091 and 1 095 nm by coupled stimulated Raman scattering [J]. ***Optics Express***, 2012, 20(25): 27838-27846.

[101] Zhang H, Chen X, Wang Q, et al. Dual-wavelength actively *Q*-switched diode-end-pumped ceramic Nd:YAG/$BaWO_4$ Raman laser operating at 1 240 and 1 376 nm [J]. ***Laser Physics Letters***, 2014, 11(10): 105806.

[102] Huang Y J, Chen Y F, Chen W D, et al. Dual-wavelength eye-safe Nd: YAP Raman laser [J]. ***Opt Lett***, 2015, 40(15): 3560-3563.

[103] Sun Y, Lee C, Zhu Z, et al. Dual-polarization balanced Yb: GAB crystal for an intracavity simultaneous orthogonally polarized multi-wavelength KGW Raman laser [J]. ***Opt Mater Express***, 2016, 6(11): 3550-3557.

[104] Tu Z H, Dai S B, Chen M T, et al. High-peak-power eye-safe orthogonally-polarized dual-wavelength Nd: YLF/KGW Raman laser [J]. ***Optics Express***, 2020, 28(6): 8802-8810.

[105] Duan Y, Sun Y, Zhu H, et al. $YVO_4$ cascaded Raman laser for five-visible-wavelength switchable emission [J]. ***Opt Lett***, 2020, 45(9): 2564-2567.

[106] Fan L, Wang X, Zhao X, et al. First-Stokes and second-Stokes multi-wavelength continuous-wave operation in Nd: $YVO_4$/$BaWO_4$ Raman laser under in-band pumping [J]. ***Chinese Optics Letters***, 2020, 18(11): 111401.

[107] Williams R J, Kitzler O, Bai Z, et al. High power diamond Raman lasers [J]. ***IEEE Journal of Selected Topics in Quantum Electronics***, 2018, 24(5): 1602214.

[108] Chen H, Bai Z, Cai Y, et al. Order controllable enhanced stimulated Brillouin scattering utilizing cascaded diamond Raman conversion [J]. ***Applied Physics Letters***, 2023, 122(9): 092202.

[109] Bai Zhenxu, Yang Xuezong, Chen Hui, et al. Research progress of high-power diamond laser technology (*invited*) [J]. ***Infrared and Laser Engineering***, 2020, 49(12): 20201076. (in Chinese)

[110] Bai Z, Williams RJ, Kitzler O, et al. 302 W quasi-continuous cascaded diamond Raman laser at 1.5 microns with large brightness enhancement [J]. ***Optics Express***, 2018, 26(16): 19797-19803.

[111] Mckay A, Liu H, Kitzler O, et al. An efficient 14.5 W diamond Raman laser at high pulse repetition rate with first (1240 nm) and second (1485 nm) Stokes output [J]. ***Laser Physics Letters***, 2013, 10(10): 105801.

[112] Bai Z, Williams R J. Kitzler O, et al. Diamond Brillouin laser in the visible [J]. ***APL Photonics***, 2020, 5(3): 031301.

[113] Dashkevich V I, Orlovich V A. Ring solid-state Raman laser at 1 538 nm [J]. ***Laser Physics Letters***, 2021, 8(9): 661-667.

[114] Kitzler O, Lin J, Pask H M. et al. Single-longitudinal-mode ring diamond Raman laser [J]. ***Opt Lett***, 2017, 42(7): 1229-1232.

[115] Hou Junyan, Shu Shijiang, Wang Yuefeng, et al. High power high beam quality LD dual-end-pumped Z folded resonator Nd:$YVO_4$ laser [J]. ***Acta Optica Sinica***, 2010, 30(8): 2299-2305. (in Chinese)

[116] Sun Y, Li M, Kitzler O, et al. Stable high-efficiency continuous-wave diamond Raman laser at 1 178 nm [J]. ***Laser Physics Letters***, 2022, 19(12): 125001.

[117] Li M, Sun Y, Jiang H, et al. Secondary Raman and Brillouin mode suppression in two-and three-mirror-cavity diamond

Raman lasers [J]. *Optics Express*, 2023, 31(5): 8622-8631.

[118] Warrier A M, Lin J, Pask H M, et al. Highly efficient picosecond diamond Raman laser at 1240 and 1485 nm [J]. *Optics Express*, 2014, 22(3): 3325-3333.

[119] Li M, Kitzler O, Spence D J. Investigating single-longitudinal-mode operation of a continuous wave second Stokes diamond Raman ring laser [J]. *Optics Express*, 2020, 28(2): 1738-1744.

[120] Li M, Kitzler O, Mildren R P, et al. Modelling and characterisation of continuous wave resonantly pumped diamond Raman lasers [J]. *Optics Express*, 2021, 29(12): 18427-18436.

[121] Frank M, Smetanin S N, Jelinek M, et al. Multiwavelength, picosecond, synchronously pumped, $Pb(MoO_4)_{0.2}(WO_4)_{0.8}$ Raman laser oscillating at 12 wavelengths in a range of 1 128-1 360 nm [J]. *Opt Lett*, 2021, 46(20): 5272-5275.

[122] Granados E, Pask H M, Esposito E, et al. Multi-wavelength, all-solid-state, continuous wave mode locked picosecond Raman laser [J]. *Optics Express*, 2010, 18(5): 5289-5294.

[123] Parrotta D C, Kemp A J, Dawson M D, et al. Tunable continuous-wave diamond Raman laser [J]. *Optics Express*, 2011, 19(24): 24165-24170.

[124] Cai Y, Gao F, Chen H, et al. Continuous-wave diamond laser with a tunable wavelength in orange-red wavelength band [J]. *Optics Communications*, 2023, 528: 128985.

[125] Casula R, Penttinen J P, Guina M, et al. Cascaded crystalline Raman lasers for extended wavelength coverage: continuous-wave, third-Stokes operation [J]. *Optica*, 2018, 5(11): 1406-1413.

[126] Wang X, Wang X, Zheng Z, et al. 1164.4 nm and 1174.7 nm dual-wavelength $Nd:GdVO_4/Cr^{4+}:YAG/YVO_4$ passively *Q*-switched Raman microchip laser [J]. *Appl Opt*, 2018, 57(12): 3198-3204.

# Review of multi-wavelength laser technology based on crystalline Raman conversion (*invited*)

Lv Zhiwei[1,2], Liu Zhongze[1,2], Chen Hui[1,2], Jin Duo[1,2], Hao Xin[1,2], Fan Wenqiang[1,2], Wang Yulei[1,2], Bai Zhenxu[1,2*]

(1. Center for Advanced Laser Technology, Hebei University of Technology, Tianjin 300401, China;
2. Hebei Key Laboratory of Advanced Laser Technology and Equipment, Tianjin 300401, China)

**Abstract:**

**Significance** Multi-wavelength lasers that can simultaneously or alternately output different wavelengths have various applications in optoelectronic countermeasures, LiDAR, and medical treatment. However, achieving controllable and efficient multi-wavelength laser radiation is challenging due to the limitations of the emission spectrum and intensity of the laser materials. Nonlinear optical frequency conversion technology, especially stimulated Raman scattering (SRS), is an effective way to expand the laser wavelength range and enhance the laser power. SRS is a third-order nonlinear optical effect that shifts the frequency of the pump through molecular or lattice vibrations in the medium. Raman lasers can obtain high-power, high-beam-quality, and multi-wavelength laser output by utilizing the characteristics of phase conjugation, amplification, and cascade conversion of SRS. This paper introduces the basic principles of SRS and cascaded Raman conversion, summarizes the classification and structure of typical crystal Raman lasers, and reviews the current status, challenges, and opportunities of multi-wavelength laser technology based on crystal Raman conversion.

**Progress** The working principle of the stimulated Raman scattering (Fig.2) and the excitation principle of cascaded Raman scattering (Fig.3) are first outlined in this article. Then the basic structure of Raman lasers was discussed (Fig.4), which can be classified into intracavity and external cavity based on the location of the Raman gain medium relative to the laser working material. A special case of intracavity Raman lasers is self-Raman lasers, where the laser working material and the Raman gain medium are the same. Next, the characteristics of different types of Raman gain media, including gas, liquid, and solid are analyzed. Among them, Raman crystals are regarded as a promising medium for multi-wavelength lasers due to their advantages such as high gain, compact structure, and good stability. Typical crystal Raman gain media were compared and their parameters are summarized (Tab.1). Finally, the current research status of multi-wavelength crystalline Raman lasers as well as their features are summarized. Based on the above research status, it is not difficult to find that linear cavities are still the most commonly used resonant cavity structure for generating multi-wavelength Raman lasers, and pulse lasers account for the highest proportion of the research. In addition, compared to intracavity Raman oscillators, external cavity Raman oscillators exhibit higher average and peak power, demonstrating stronger power scalability. Although microcavity Raman lasers currently have low output power and conversion efficiency, they have the characteristics such as high repetition rate and miniaturization.

**Conclusions and Prospects** In conclusion, research on multi-wavelength lasers based on crystalline Raman conversion has made significant progress in the past decade, with the discovery of new crystals, structures, and wavelengths. The use of new crystal materials such as diamond has led to a remarkable performance in power enhancement, wavelength expansion, and miniaturization of multi-wavelength Raman lasers. Future research should focus on optimizing pump parameters and oscillator design to improve conversion efficiency, expand multi-wavelength lasers' output spectral range, and improve thermal management under high-power operation to enhance system stability and beam quality. With these advancements, we can expect that multi-wavelength solid-state lasers based on crystalline Raman conversion will play a major role in future applications.

**Key words:** stimulated Raman scattering; multi-wavelength laser; Raman crystal; cascaded conversion; Raman oscillator

**Funding projects:** National Natural Science Foundation of China (61927815); Natural Science Foundation of Tianjin (22JCYBJC01100, 20JCZDJC00430); Program of State Key Laboratory of Quantum Optics and Optical Quantum Devices (KF202201); Funds for Basic Scientific Research of Hebei University of Technology (JBKYTD2201)